

7-12-2014

COMPARISON OF E. COLI AND Y. PESTIS LPS TLR4 TIME COURSE ON P388D1 MACROPHAGES USING FLUORESCENT CONJUGATED ANTIBODIES

Julia Kleven

Follow this and additional works at: https://digitalrepository.unm.edu/ece_etds

Recommended Citation

Kleven, Julia. "COMPARISON OF E. COLI AND Y. PESTIS LPS TLR4 TIME COURSE ON P388D1 MACROPHAGES USING FLUORESCENT CONJUGATED ANTIBODIES." (2014). https://digitalrepository.unm.edu/ece_etds/140

This Thesis is brought to you for free and open access by the Engineering ETDs at UNM Digital Repository. It has been accepted for inclusion in Electrical and Computer Engineering ETDs by an authorized administrator of UNM Digital Repository. For more information, please contact disc@unm.edu.

Julia Kleven

Candidate

Electrical and Computer Engineering

Department

This thesis is approved, and it is acceptable in quality and form for publication:

Approved by the Thesis Committee:

Edl Schamiloglu , Chairperson

Jerilyn Timlin

Salvador Portillo

**COMPARISON OF *E. COLI* AND *Y. PESTIS* LPS TLR4 TIME
COURSE ON P388D1 MACROPHAGES USING
FLUORESCENT CONJUGATED ANTIBODIES**

by

JULIA KLEVEN

**BACHELORS OF SCIENCE
BIOMEDICAL ENGINEERING
BOSTON UNIVERSITY, 2011**

THESIS

Submitted in Partial Fulfillment of the
Requirements for the Degree of

**Masters of Science
Electrical Engineering**

The University of New Mexico
Albuquerque, New Mexico

May, 2014

ACKNOWLEDGMENTS

I would like to thank everyone who helped me complete this thesis. I would never have made it through without the help from everyone at the University of New Mexico, Sandia National Labs, and my friends and family.

I would like to thank Professor Edl Schamiloglu, my advisor and chair, for all his help getting through this difficult program. I have been so honored to be part of your Applied EM group at UNM and have learned so much from you as well as the other wonderful people in the group. I would also like to thank Professor Sal Portillo for giving me the opportunity to do this collaboration with Sandia.

I want to give my deepest gratitude to all the people at Sandia for all of their help throughout this project. Much of the research presented here would not have been possible without their knowledge and expertise. I especially want to thank Dr. Jerilyn Timlin and Dr. Amanda Carroll-Portillo. Without your patience, understanding, and guidance I would have never made it through. Thank you for all your encouragement.

Finally, I want to thank my friends and family for all their love and support. A special thanks to my mom and Brian. I wouldn't have made it without you.

**Comparison of *E. coli* and *Y. pestis* LPS TLR4 Time Course on P388D1
Macrophages using Fluorescent Conjugated Antibodies**

By

Julia Kleven

B.S., Biomedical Engineering, Boston University, 2011

M.S., Electrical Engineering, University of New Mexico, 2014

ABSTRACT

The innate immune system enables cellular response to infectious agents, and protein interactions are essential for this response. However, the protein interactions involved in cellular response to pathogens are not completely understood. Clarifying the manner in which proteins bind and respond to infectious agents is necessary for development of potential therapeutics or preventative measures.

Fluorescent probes and fluorescent microscopy are used to aid in the visualization of these components, but proteins associated with or spanning the cellular membrane are on the nanometer scale, smaller than some microscopes can image, which makes it difficult to accurately localize the proteins of interest. To further the understanding of protein dynamics, a higher resolution form of optical microscopy had to be developed that allowed for multi-component cellular imaging without the need for harsher fixatives like those required for electron microscopy. To this end, optical super resolution techniques rely on the blinking attributes of fluorophores currently utilized in protein labeling in conjunction with specialized post processing to enable sub-diffraction limit

localization. These techniques allow the visualization of protein dynamics on the scale in which they occur.

It is through these methods that we clarify the protein interactions involved in response to the extracellular stimuli provided by a variety of bacterial lipopolysaccharides (LPS), known stimulants of the innate immune system. It has been shown that LPS-induced TLR4 dimerization and clustering correlate to an appropriate innate immune response. Imaging the degree of TLR4 clustering after exposure to different gram negative LPS can further the understanding of TLR4 pathway dynamics. By studying the internalization of TLR4, it can be determined whether cells have had adequate time to react and form clusters as a result of being exposed to LPS. These experiments will focus on imaging the LPS from *E. coli* as well as of *Y. pestis* 21C on several microscopes.

TABLE OF CONTENTS

ACKNOWLEDGEMENTS	iii
Abstract	iv
List of Figures	vii
Thesis Outline	2
Chapter 1	1
Introduction	1
1.1 Background	1
Chapter 2	3
Review of Related Literature	3
2.1 Cellular Signaling – TLR4 Pathway.....	3
2.2 Microscopes	6
2.2.1 Wide-field Microscope.....	6
2.2.2 Confocal Microscopes.....	7
2.2.3 TIRF Microscopy.....	10
2.2.4 dSTORM Microscopy.....	11
Chapter 3	14
Methods	14
3.1 Biology Methods	14
3.2 Upright Olympus BX51 Microscope Setup.....	15
3.3 Image Analysis.....	16
Chapter 4	21
Results	21
4.1 Atto 532 Labeled Antibody	21
4.2 A488 Labeled Antibody.....	24
4.3 Alexa Fluor 568 Labeled Antibody	26
Chapter 5	31
Discussion	31
Chapter 6	33
Conclusion and Future Experiments	33
REFERENCES	35

LIST OF FIGURES

Figure 2.1: Description of the reaction of the TLR4 pathway when exposed to <i>Y. pestis</i> 21C LPS and <i>Y. pestis</i> 37C LPS.	5
Figure 2.2: Diagram of upright wide-field microscope.	7
Figure 2.3: Diagram of a spinning disk confocal microscope.....	8
Figure 2.4: Diagram of laser scanning confocal microscope.....	9
Figure 2.5: Schematic of TIRF.....	11
Figure 2.6: Schematic of overlaid single molecule images with blinking fluorophores to produce dSTORM image.	12
Figure 3.1: Measurements that should be checked in Set Measurements menu in ImageJ.	17
Figure 3.2: Image showing area surrounding cell selected in ImageJ.	18
Figure 3.3: Original image, mask representing pixels above threshold, image with mask overlaid.	19
Figure 3.4: Original image, new mask representing pixels above 110% threshold, image with mask overlaid.	19
Figure 4.1: Cells labeled with a 1:250 dilution of 532 labeled antibodies imaged on laser scanning confocal microscope and unlabeled control cells showing the autofluorescence.	22
Figure 4.2: Cells labeled with a 1:100 dilution of 532 labeled antibodies imaged on laser scanning confocal microscope and unlabeled control cells showing the autofluorescence.	23
Figure 4.3: Cells labeled with a 1:100 dilution of 532 labeled antibodies imaged with TIRF microscopy and unlabeled control cells showing the autofluorescence.	24
Figure 4.4: Cells labeled with a 1:100 dilution of A488 a-TLR4 imaged on spinning disk confocal microscope and unlabeled control cells showing the autofluorescence.	25
Figure 4.5: Cells labeled with a 1:25 dilution of 488 labeled antibodies imaged on laser scanning confocal microscope and unlabeled control cells showing the autofluorescence.	26
Figure 4.6: A. P388D1 cells reacted with <i>E. coli</i> LPS for one hour and labeled with 568 antibody. These cells were imaged on the upright microscope. B. Control cells imaged on upright microscope to determine the amount of autofluorescence contributing to the signal. C. DIC image of control cells imaged on upright microscope to determine the amount of autofluorescence contributing to the signal.	27

Figure 4.7: A. P388D1 cells incubated with *Y. pestis* 21C LPS for one hour and labeled with a-TLR4 A568 and imaged on an upright wide-field microscope with an oil 100x objective. B. Control cells were treated similarly as samples labeled with a-TLR4 A568 and imaged using the same conditions to determine levels of autofluorescence. C. DIC image of control cells to determine where the cellular membrane is when calculating autofluorescence. 28

Figure 4.8: Rate of LPS internalization for *E. coli* and *Y. pestis* 21C..... 29

Chapter 1

Introduction

1.1 Background

The eukaryotic cell membrane consists of a phospholipid bilayer with proteins embedded in it. These proteins have specialized functions and interactions that allow for the cell to take in nutrients, deposit waste, and identify possible infectious agents. The signal-transduction events the cell employs to identify and respond to these infectious agents are collectively known as the innate immune response. The innate immune system enables cellular response to infectious agents, and protein interactions are essential for this response. However, the protein interactions involved in cellular response to pathogens are not completely understood. Clarifying the manner in which proteins bind and respond to infectious agents is necessary for development of potential therapeutics or preventative measures.

Fluorescent probes and fluorescent microscopy are used to aid in the visualization of these components, but proteins associated with or spanning the cellular membrane are on the nanometer scale, smaller than most wide-field microscopes can image, which makes it difficult to accurately localize the proteins of interest. To further the understanding of protein dynamics, a higher resolution form of optical microscopy had to be developed that allowed for multi-component cellular imaging without the need for harsher fixatives like those required for electron microscopy. To this end, optical super resolution techniques rely on the blinking attributes of fluorophores currently utilized in protein labeling in conjunction with specialized post processing to enable sub-diffraction limit localization. These techniques allow the

visualization of protein dynamics on the scale in which they occur. It is through these methods that we clarify the protein interactions involved in response to the extracellular stimuli provided by a variety of bacterial lipopolysaccharides (LPS), known stimulants of the innate immune system.

1.2 Thesis Outline

This thesis describes the results of imaging internalization events seen when eukaryotic TLR4 has been exposed to gram negative LPS from *Escherichia coli* (*E. coli*) and *Yersinia pestis* (*Y. pestis*). This thesis is organized as follows: Chapter 1 discusses a brief introduction for the need to image the membrane proteins associated with innate immunity. Chapter 2 describes more detail about the biological pathways imaged and microscopes used. Chapter 3 discusses the methods used to obtain the results found, including the microscope setups, the sample preparation protocols, and the image analysis. Chapter 4 examines the results found in the images. Chapter 5 discusses the possible implications and shortcomings found in Chapter 4. Finally, Chapter 6 presents a summary of this thesis and recommendations for future work.

Chapter 2

Review of Related Literature

This chapter contains descriptions of the biological pathways that are the focus of this work as well as the microscopes used to image them. The Bioenergy and Defense Technologies Department at Sandia National Laboratories (SNL) owns and maintains the systems used and described in this thesis. The biological and chemical materials needed to perform these experiments are also located in this department.

2.1 Cellular Signaling – TLR4 Pathway

The innate immune system provides initial responses to invading pathogens. The cells that are primarily involved are able to recognize pathogen-associated molecular patterns (PAMPs). PAMPs are structural motifs found in bacteria, viruses and fungi that are recognized by pattern recognition receptors like toll-like receptors (TLRs). Some of the PAMPs that stimulate the TLR4 pathway include lipopolysaccharide (LPS) from Gram-negative bacteria, fusion protein from respiratory syncytial virus and the envelope protein from mouse mammary tumor virus. LPS is part of the outer membrane of Gram-negative bacteria and is a major stimulant of the innate immune system. It has three components: lipid A, a core oligosaccharide, and an O side chain. Lipid A is the main PAMP to excite an immune response to the TLR4 pathway and initiate cell-mediated responses including microbicidal effects and cytokine release.

[1]

It has been shown that LPS-induced TLR4 dimerization and clustering correlate to an appropriate innate immune response. [2] Therefore, imaging the degree of TLR4 clustering after exposure to different gram negative LPS can further the understanding of TLR4 pathway dynamics. By studying the internalization of TLR4, it can be determined whether cells have had adequate time to react and form clusters as a result of being exposed to LPS. Future experiments will focus on imaging the LPS from *E. coli*, as well as two different temperatures of *Y. pestis*. *Y. pestis* changes its structure based on the temperature in which it is grown. When grown at 37 degrees Celsius (37C) the LPS has a tetraacyl lipid A and is not immune stimulatory for mammalian cells. However, *Y. pestis* LPS from bacteria grown at 21 degrees Celsius (21C) has additional pentaacyl and hexaacyl lipid A structures and does produce a robust innate immune response. [3] It is hypothesized that *Y. pestis* 21C LPS will cause TLR4-oligomerization on the cell membrane in while *Y. pestis* 37C will elicit no signaling cascade. [3]

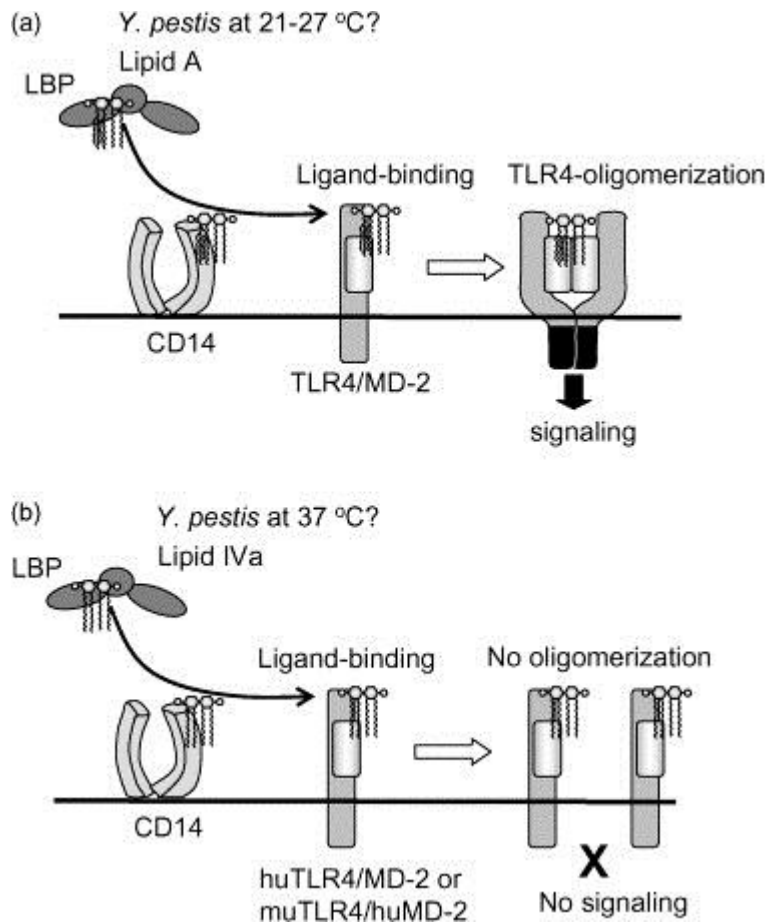


Figure 2.1 Description of the reaction of the TLR4 pathway when exposed to *Y. pestis* 21C LPS and *Y. pestis* 37C LPS. [3]

This thesis aims to study a time course of internalization of TLR4 through imaging fluorescently labeled anti-TLR4 antibodies. By using fluorescently labeled antibodies, detection of TLR4 internalization dynamics upon stimulation with different types of LPS is possible using laser scanning confocal and widefield microscopy. Results of the time course will allow the determination of LPS incubation time in higher resolution microscopes to target when TLR4 membrane dynamics in response to LPS are optimal.

2.2 Microscopes

A 100x oil objective on an upright Olympus IX 71 wide-field microscope was used to image TLR4 internalization. These results will provide additional detail to the confocal microscope, total internal reflection fluorescence (TIRF) microscope, and dual color direct Stochastic Optical Reconstruction Microscope (dSTORM) results.

2.2.1 Wide-Field Microscope

White light is sent through an excitation, in this case TRITC, filter. The specific light is then reflected off of a dichromatic mirror, through the objective, and onto the specimen. The light excites the fluorophores, causing them to emit fluorescent light. This emitted light, combined with the reflected light, is then passed back through the dichromatic mirror and barrier filters to remove the reflected wavelengths, leaving only the emitted light from the sample to be detected by a camera.

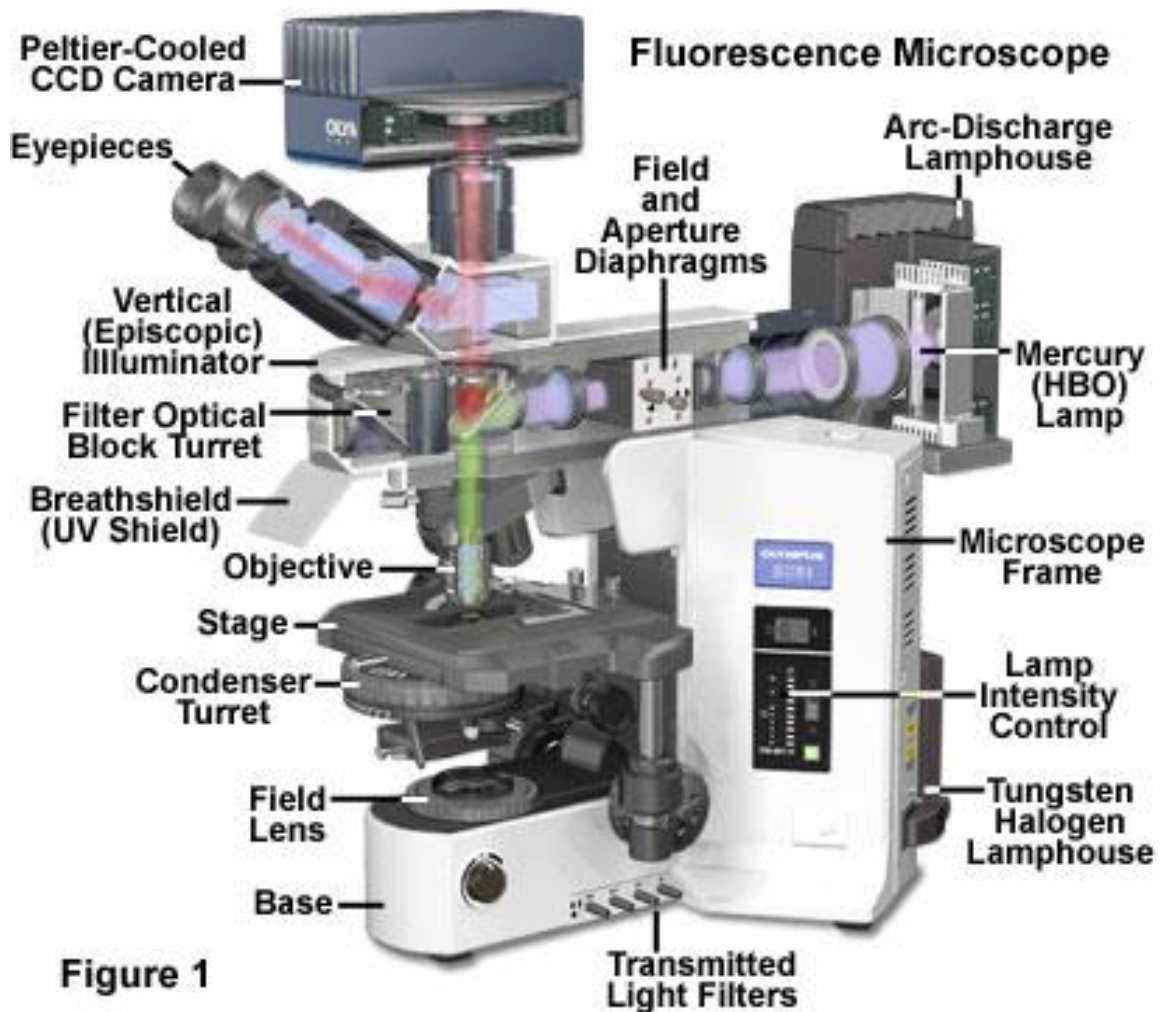


Figure 1

Figure 2.2 Diagram of upright wide-field microscope. [4]

2.2.2 Confocal Microscopes

A spinning disk confocal microscope uses a light source to scan over multiple spinning disks. The light is directed through a collector disk containing spinning micro lenses containing pinholes that send the beam down through a corresponding spinning pinhole disk and through the objective lens down onto the specimen. The light is then reflected back through the objective lens and the pinhole and sent to an EMCCD camera. An EMCCD camera is an electron-

multiplying charge-coupled device which acts as an electron multiplier. The advantages the spinning disk confocal microscope has over conventional wide-field microscopy includes the ability to remove out-of-focus signal, as the light has to be reflected through a pinhole and the light refracted at an angle contributing to noise is filtered out. Also, the confocal is able to capture information at a reduced depth and image discrete sections to create a 3D image. [5]

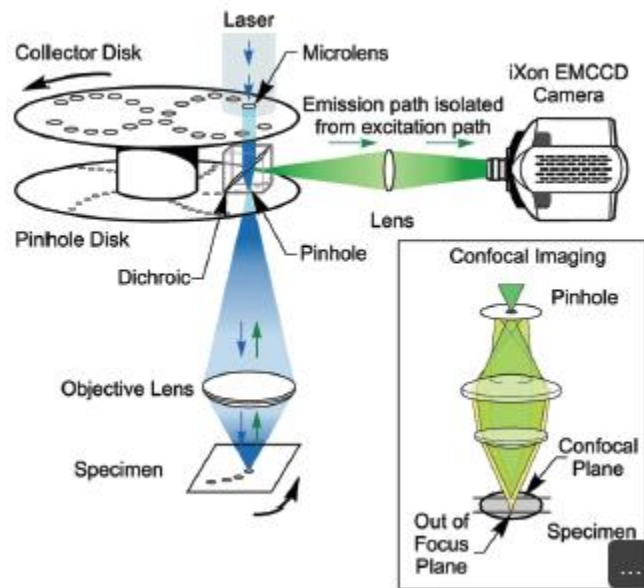


Figure 2.3 Diagram of a spinning disk confocal microscope. [5]

The spinning disk confocal microscope and the laser scanning microscope have the advantage of being able to remove out of focus light to record images of discrete depths of a sample in order to recreate a 3D image with image processing software. The laser scanning confocal microscope uses coherent light from laser excitation source is first sent through a light source pinhole aperture. The light is then sent through an excitation-filter that removes unwanted frequencies. The remaining frequencies are directed off of a dichromatic mirror and through an

objective to the focal plane of the specimen. The specimen is labeled with fluorophores that become excited when exposed to specific frequencies. As the fluorophores return to their ground state from the excited state, they fluoresce. This fluorescent signal is then directed back through the objective through an emission filter (band pass or long pass). This filter works to remove the unwanted signals (including potential laser and fluorophore bleed through). Finally, the signal is sent through a pinhole aperture and into a photomultiplier tube. The pinhole aperture filters the out of focus light rays, thereby allowing only in focus light from the focal plane of the sample to be sent to the photomultiplier tube. [6] The photomultiplier tube can be adjusted to amplify low fluorescent signals. This process is repeated as the laser beam scans the sample point by point in a raster pattern until the image is formed.

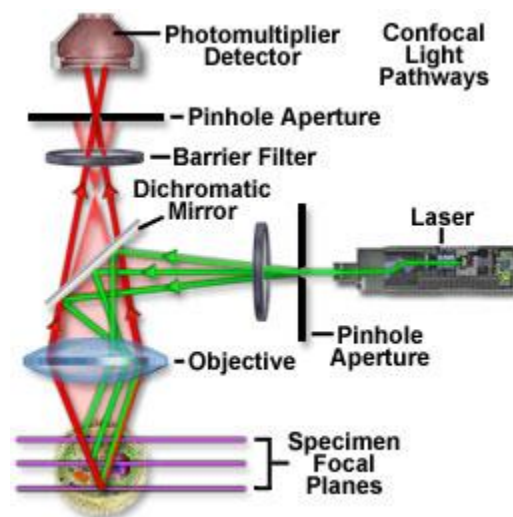


Figure 2.4 Diagram of laser scanning confocal microscope. [6]

While the axial resolution of the laser scanning confocal is higher than that of spinning disk microscope, and therefore able to provide more detailed information about intracellular organelles and their relationship to one another, the frame rate is decreased due to the laser having to illuminate each point separately to form the image. [5] The resolution of the laser

scanning confocal microscope is diffraction limited. The diffraction limit is described as the maximum point-to-point resolution that can be obtained using a light source. The equations for the lateral_{x,y} and axial_z resolutions were determined by German physicist Ernest Abbe in 1873 and later refined by Lord Rayleigh in 1896 as

$$\text{Resolution}_{x,y} = \frac{\lambda}{2NA} \quad \text{Resolution}_z = \frac{2\lambda}{NA^2}, \quad (\text{Equation 2.1})$$

where λ is the average wavelength of the transmitted light, and NA stands for the numerical aperture. The numerical aperture is the ability of the microscope objective to accept light from a range of angles and produce an amount of detail. The NA can be calculated as

$$NA = n \sin \theta, \quad (\text{Equation 2.2})$$

where n is the refractive index of the media between the sample and the objective. This is usually either water with $n = 1.33$ or immersion oil with $n = 1.51$. θ refers to the one-half angular aperture of the objective. [7] This equation comes from the idea that the images are composed of diffraction-limited spots with varying intensity. If the two spots are located closer than the axial resolution, the microscope will not be able to distinguish whether there are two fluorophores or just one higher intensity fluorophore. [8]

2.2.3 TIRF Microscopy

In total internal reflection fluorescence (TIRF) microscopy, fluorophores are excited with a fiber coupled solid-state laser of a certain wavelength. The laser beam is directed at the sample at an angle that is greater than the critical angle and moves from a higher refractive index to a lower refractive index. This causes the beam to reflect internally resulting in production of an

evanescent wave at the coverslip interface. This evanescent wave illuminates approximately 200 nm into the sample, thus exciting only the fluorophores near the interface. This minimizes the signal from regions above the membrane, increasing the signal-to-noise ratio and enhancing the axial resolution. The resulting fluorescence is detected on an EMCCD camera. [9] This method of microscopy was able to break the diffraction limit in the axial direction and is extremely useful for viewing cellular membranes. However, it is still limited by optical diffraction in the lateral dimension.

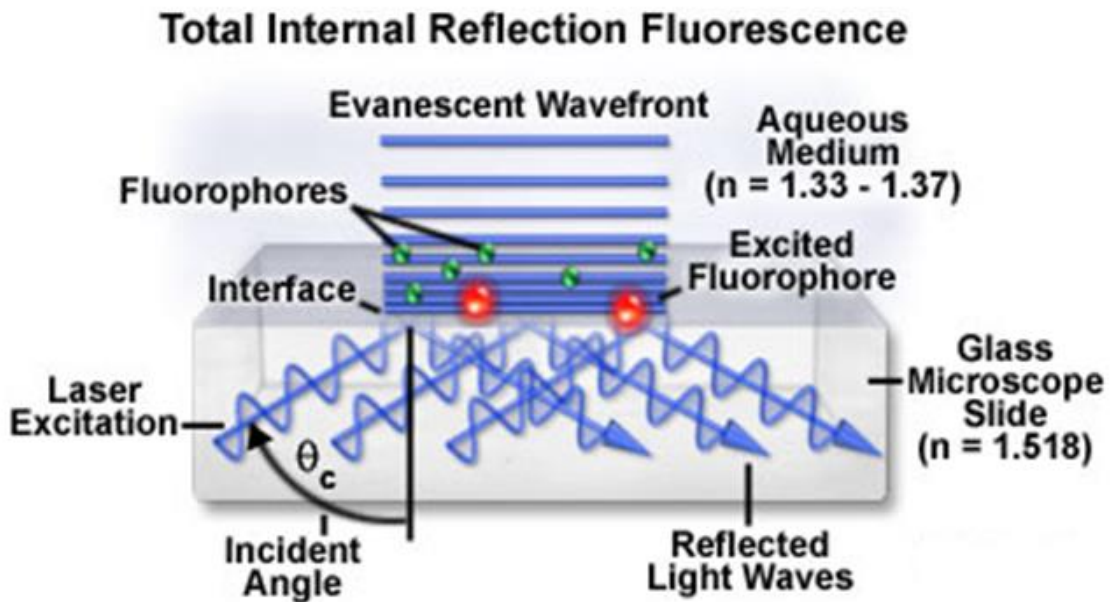


Figure 2.5 Schematic of TIRF. [10]

2.2.4 dSTORM Microscopy

Direct stochastic optical reconstruction microscopy (dSTORM) is a type of optical super-resolution microscopy that can break the diffraction limit in the lateral dimension. dSTORM

uses TIRF excitation of the sample to reduce the amount of background from above the membrane. It collects a series of images of single molecules that are then individually localized, leading to lateral spatial resolutions on the order of 40 nm. dSTORM requires compilation of thousands of TIRF images, at different time points when different molecules are fluorescing, to produce one image. [12] The molecules are excited a few at a time using an oxygen scavenging system and thiol compound which reacts with the triplet state of the fluorophore generating a non-fluorescent reduced state (dark state). The molecule is then oxidized with molecular oxygen to recover the fluorescent state allowing the molecules to blink at different times. [13] This allows for higher lateral resolution as, when two molecules are closer than the TIRF lateral resolution but blink at different times, the EMCCD is able to detect two distinct fluorophores instead of one high intensity fluorophore. dSTORM images are able to achieve a spatial resolution of 30 nm. [14]

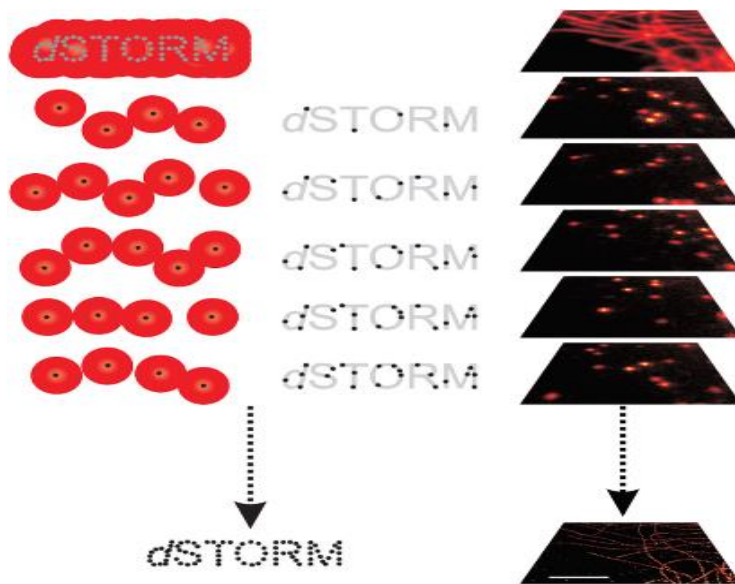


Figure 2.6 Schematic of overlaid single molecule images with blinking fluorophores to produce dSTORM image. [15]

While dSTORM microscopy has the advantage of breaking the diffraction limit in the lateral direction, some drawbacks to this type of microscopy include the presence of the very stochasticity that makes it work. Stochastic switching of the fluorophores from an illuminated state to a dark state creates the possibility that not all the fluorophores have been imaged in their illuminated state.

Chapter 3

Methods

In order to study the evolution over time of internalization of the labeled TLR4 by P388D1 macrophages when exposed to *E. coli* lipopolysaccharides, fluorescent antibody tags as well as a variety of microscopes were used.

3.1 Biology Methods

P388D1 macrophage cells (ATCC TIB-63) were cultured at 37C in a CO₂ environment (5%) using Roswell Park Memorial Institute (RPMI) media (ATCC) supplemented with 10% fetal bovine serum (Gibco)(RPMI-10), L-glutamine (1%) and Penicillin-Streptomycin (1%). For experiments, cells were seeded on #1 glass coverslips, previously cleaned with piranha solution (12 M H₂SO₄ and 30% H₂O₂, 1:3), at 4×10^5 cells mL⁻¹.

Anti-mouse TLR4 (α -TLR4; eBioscience, Clone UT41) was either purchased labeled with Alexa Fluor 488, or was labeled in lab with Atto 532 (Sigma) per manufacturer instructions. A different α -TLR4 was purchased from Abcam and labeled in lab with Alexa Fluor 568 (Life Technologies) per manufacturer instructions. These antibodies were added at different dilutions to samples as described in later sections. LPS from *E. coli* was purchased from Sigma, catalog number L-3129. LPS from *Y. pestis* (21C) was purified as previously described. [16] Live cell imaging buffer, composed of a balance of salts and proteins in a HEPES based buffer (1x Hanks,

10 mM HEPES, 0.05% Bovine Serum Albumin, 5 mM Glucose, 0.7 mM MgSO₄, 0.2 mM CaCl₂, and 0.13% NaHCO₃), helped to maintain cells during the labeling procedure.

Prior to endotoxin exposures, P388D1 cells were washed with RPMI-10. Samples were exposed to LPS (100 nM) derived from *E. coli* diluted in RPMI-10. Cells were allowed to interact with the LPS for the respective 5 minutes, 10 minutes, 30 minutes, or 1 hour time course at 37C, 5% CO₂. Immediately after, cells were washed with live cell imaging buffer. 40 μL of Fc block (Innovex NB309-15) were added to the cells for 5 minutes while on ice. The Fc block was then dabbed off, and labeled antibody with a solution of live cell imaging buffer and 0.02% saponin was added. Saponin was used to perforate the cellular membrane at a low level to give α-TLR4 antibodies access to intracellular TLR4. The cells were allowed to incubate with the labeled antibody for 30 minutes on ice. They were then washed with the live cell imaging buffer, and 100 μL of a 4% paraformaldehyde buffered solution was added and allowed to react for 15 minutes at room temperature to fix the cells. The cells were then washed with 1x PBS and mounted onto a slide using Prolong Gold.

3.2 Upright Olympus BX51 Microscope Setup

Percent internalization was determined using samples that were imaged on the Olympus BX51 Upright Microscope with a 100x, 1.3 NA oil objective. Samples were illuminated using a mercury lamp and imaged using an Infinity 3 color camera (Lumenera Corporation). The associated Infinity Capture Software was used for image acquisition, and was set to a 16-bit output. The gain was 3 for the *E. coli* trials and exposure time was 300 ms, whereas the *Y. pestis* 21C trials had a gain of 12 and an exposure time of 750 ms due to their differences in degree of

label of the antibodies. Finally, a differential interference contrast (DIC) image was taken. This is an image taken with the lamp on to illuminate the shadows from the surfaces of the cell.

3.3 Image Analysis

Images of 30 unlabeled cells were used as the control for cellular autofluorescence. Additionally, a set of cells labeled with the antibody but not reacted with any LPS was used as a control to determine membrane labeling versus internalized label. At least 30 cells of each time point and control were analyzed. To determine the locations of a fluorescent label, only pixels with intensity greater than the average and the three times the standard deviation auto fluorescent signal were considered a fluorescent tag.

Image analyses were performed using ImageJ [17] to determine the amount of internalized TLR4 under different experimental conditions. Masks were first constructed in order to determine the autofluorescent signal to subtract from the TLR4- labeled images. An image of an unlabeled control cell was subjected to the Image-color-split channels command to isolate the red channel, the correct channel for the TRITC filter used to localize the anti- TLR4 antibody. Next, an area that was not part of the cell was selected using the DIC image. This resulted in a background fluorescence value. Background relates to the part of the image that does not contain a cell. To obtain a numerical value for background the analyze-measure command was used with the set measurements to have area, mean grey value, standard deviation, and limit to threshold checked.

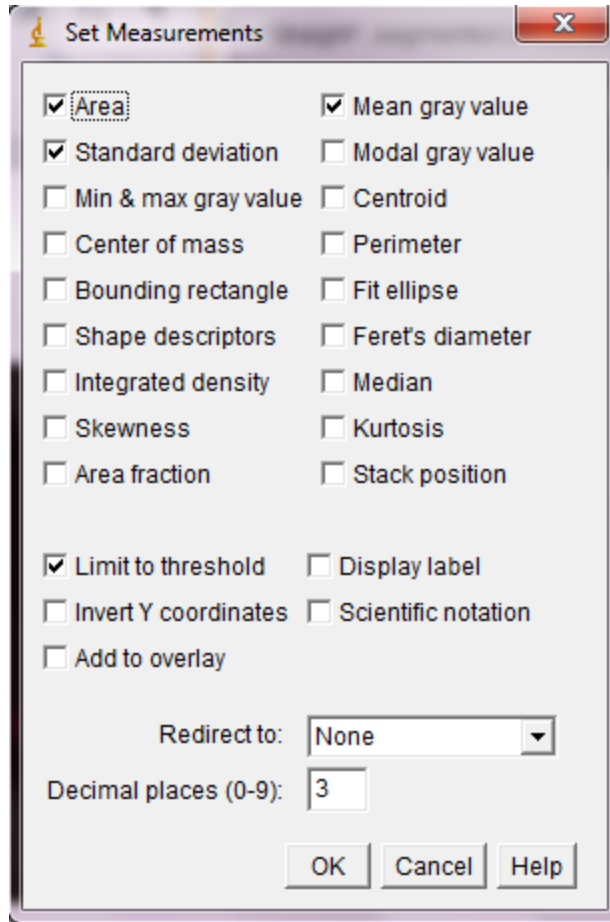


Figure 3.1 Measurements that should be checked in Set Measurements menu in ImageJ.

The background value was obtained by adding the mean grey value to three times the standard deviation. Then an area around the cell was selected as shown in Figure 3.2.

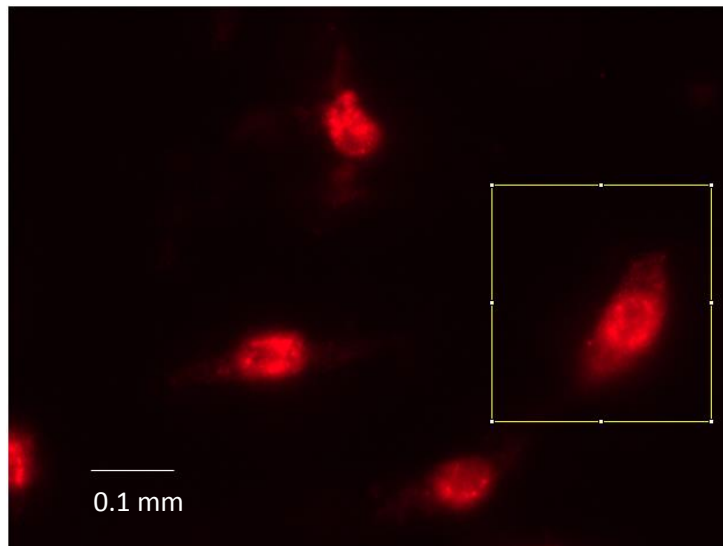


Figure 3.2 Image showing area surrounding cell selected in ImageJ.

The analyze-measure command was used to record the total area of the cell, mean intensity, and standard deviation. Once this had been performed on 30 cells, the mean background was subtracted from the mean intensity of the cell in order to find the mean autofluorescence. The total autofluorescence was considered the mean autofluorescence added to three times its standard deviation.

To determine the amount of internalization of the labeled antibody, the channels were split so only the red TRITC image was used. As before, the background levels were determined by selecting an area that is not part of any cell, using the DIC images to confirm. The analyze-measure command was used to obtain the area, mean grey value and standard deviation. These items as well as limit to threshold were still checked in set measurements. The threshold was calculated by adding the mean background to three times its standard deviation and the total autofluorescence calculated from the unlabeled cells previously. The threshold of the image was set to this value. An area around a cell was selected and the analyze-measure command was used to get the average fluorescence and area. These values only included pixels with intensities

greater than the autofluorescence and the background. The threshold was adjusted to 110% of the previous threshold and used the analyze-measure command to obtain the average fluorescence and area. The number of pixels above 110% threshold was divided by the number of pixels above the threshold to calculate the amount of internalization.

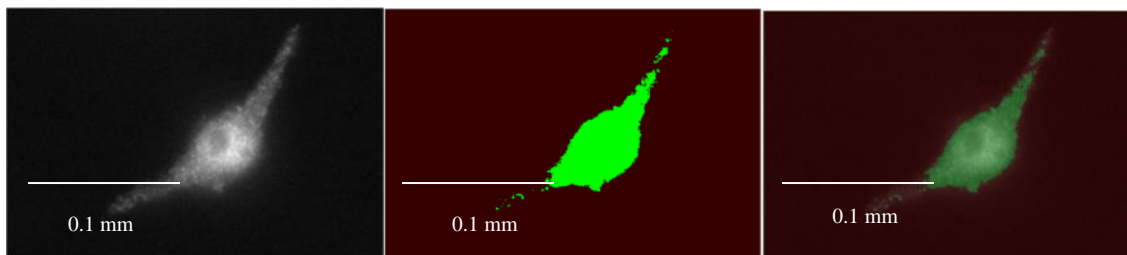


Figure 3.3 From left to right: Original image, mask representing pixels above threshold, image with mask overlaid.

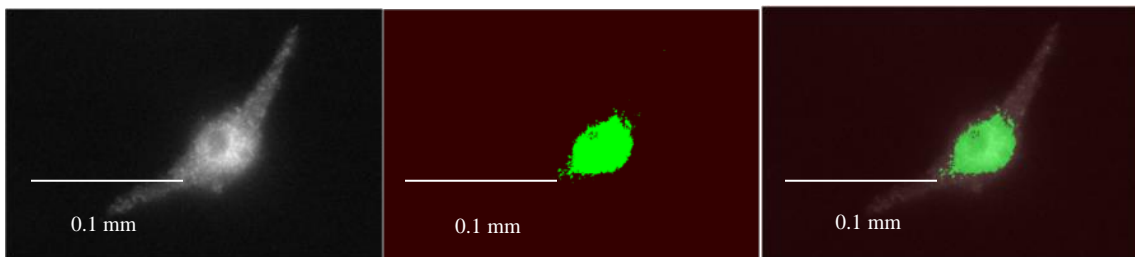


Figure 3.4 From left to right: Original image, new mask representing pixels above 110% threshold, image with mask overlaid.

The images were analyzed by building masks in ImageJ. These masks relied on thresholds to count only pixels above background and autofluorescence. The first set of masks seen in Figure 3.1 shows all pixels that were above the threshold added to three times the standard deviation. These images represent labeled antibodies both on the cell and inside the cell. The masks seen in Figure 3.2 show the pixels at 110% the original threshold. [18] Since the image had been taken in the plane of the nucleus, the organelles surrounding the nucleus will

emit higher level of autofluorescence causing the area surrounding the nucleus to be brighter. By raising the threshold 10%, the mask was able to filter the fluorophores that were located on the membrane from those that had been internalized by the cell.

Chapter 4

Results

To determine the rate of internalization of TLR4 when exposed to *E. coli* LPS, three different fluorescent dyes were used. The Atto 532 label was tried because it had been used previously in the dSTORM imaging. [2] The 488 label was used because it came already conjugated to the anti-TLR4 antibody. Finally, the 568 label was used as it fluoresced at a frequency that had less signal masking from cellular autofluorescence. Once the Atto 568 dye was chosen, the cells were reacted with either *E. coli* LPS or *Y. pestis* LPS and the rate of internalization was determined.

4.1 Atto 532 Labeled Antibody

The focus of this project was to determine whether TLR4 bound to either *E. coli* or *Y. pestis* LPS was internalized by 30 minutes, a relevant timepoint for TLR4 clustering and signaling after stimulation as previously published. [2] The previous publication used a 1:250 dilution of α -TLR4 Atto-532, so this was the first experiment tried.

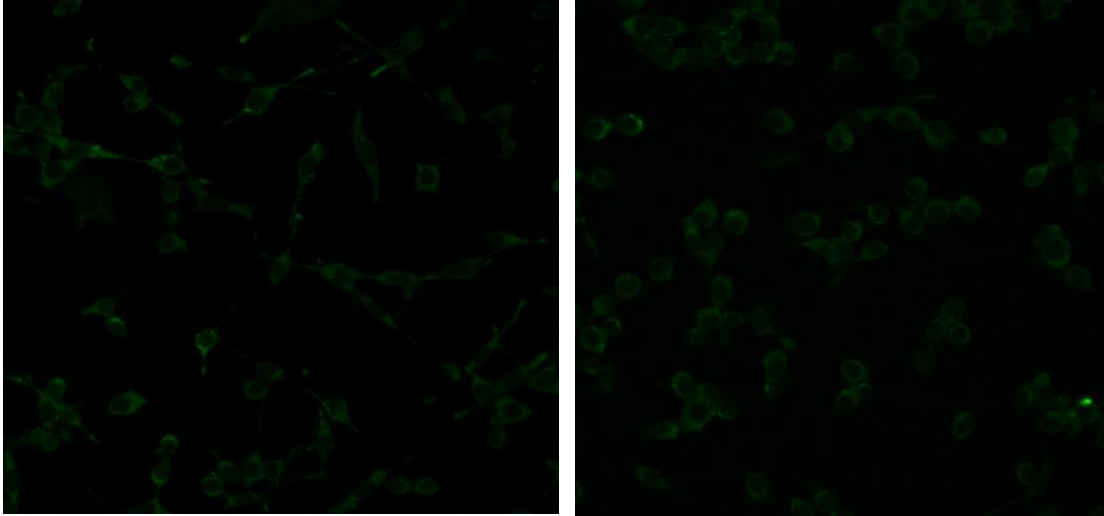


Figure 4.1 On the left cells labeled with a 1:250 dilution of 532 labeled antibodies imaged on laser scanning confocal microscope. On the right are the unlabeled control cells showing the autofluorescence.

The cells were labeled on a dish of ice to cool them for 30 minutes with 1:250 α -TLR4 Atto532, then imaged with the laser scanning confocal. A 1:100 dilution of α -TLR4 Atto532 was also performed to increase the amount of signal seen in the images.

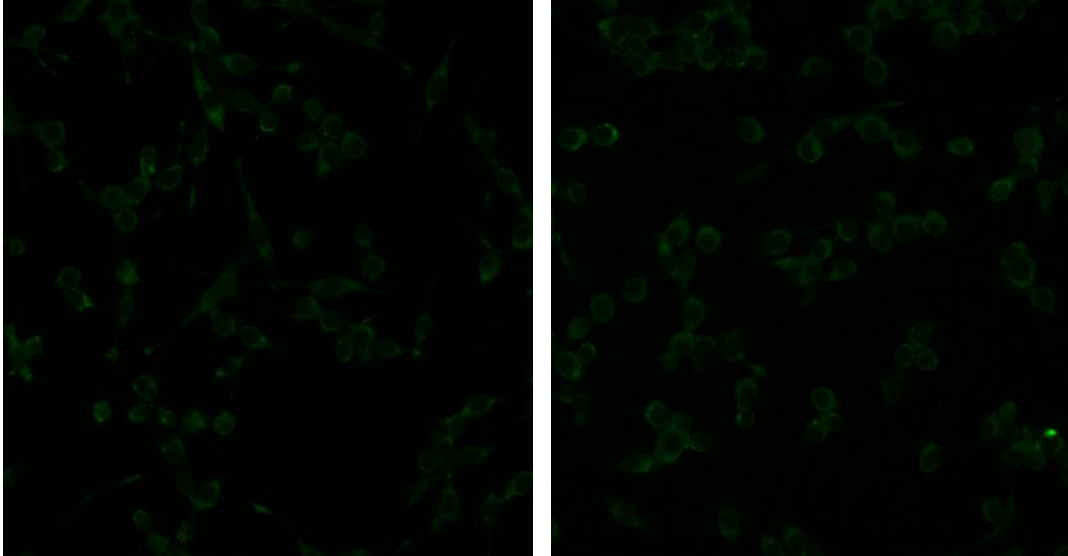


Figure 4.2 On the left cells labeled with a 1:100 dilution of 532 labeled antibodies imaged on laser scanning confocal microscope. On the right are the unlabeled control cells showing the autofluorescence.

It was hypothesized that these cells had been labeled, so a 1:200 dilution of α -TLR4 Atto532 was reacted with cells subsequent to a 1 hour activation with *E. coli* LPS. No labeling was seen in this study, so a 1:100 dilution of α -TLR4 Atto532 was reacted with the cells. Imaging of cells from this experiment was attempted in TIRF, as seen in Figure 4.3.

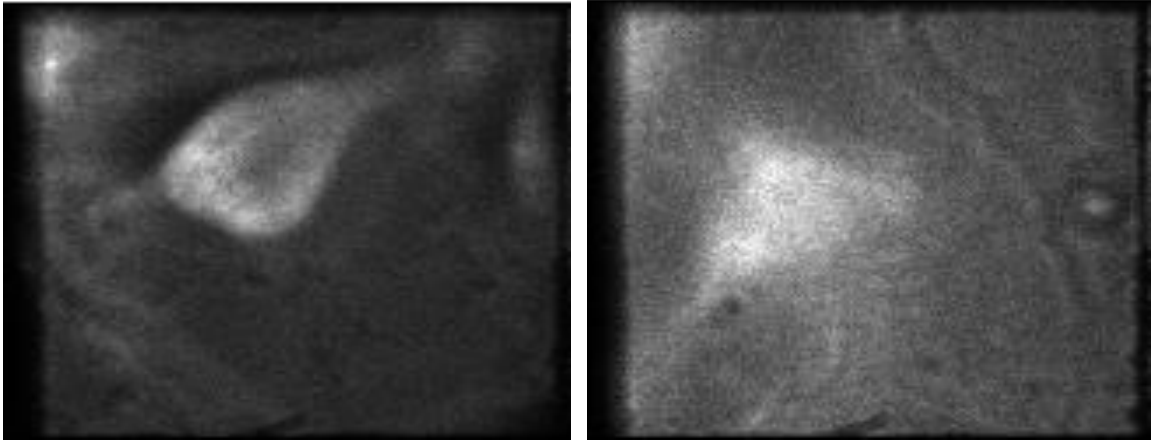


Figure 4.3 On the left cells labeled with a 1:100 dilution of 532 labeled antibodies imaged with TIRF microscopy. On the right are the unlabeled control cells showing the autofluorescence.

Hyperspectral imaging and analysis was performed on these samples. P388D1 macrophages present a high level of autofluorescence in the same filter that α -TLR4 Atto532 imaging was being performed. Hyperspectral microscopy images all of the wavelengths in a sample and allows for analysis and localization of specific fluorescent signatures. Hyperspectral results demonstrated that no Atto532 was present on the cells. It is possible the drying of the sample between TIRF imaging and hyperspectral imaging resulted in loss of fluorescent label.

4.2 A488 Labeled Antibody

To confirm the possibility that the antibodies themselves were no longer functional, new AlexaFluor 488 (A488) conjugated α -TLR4 (eBioscience) antibody was ordered. Labeling of resting cells (not treated with LPS) with A488 α -TLR4 was performed for either 30 minutes or 1 hour on ice.

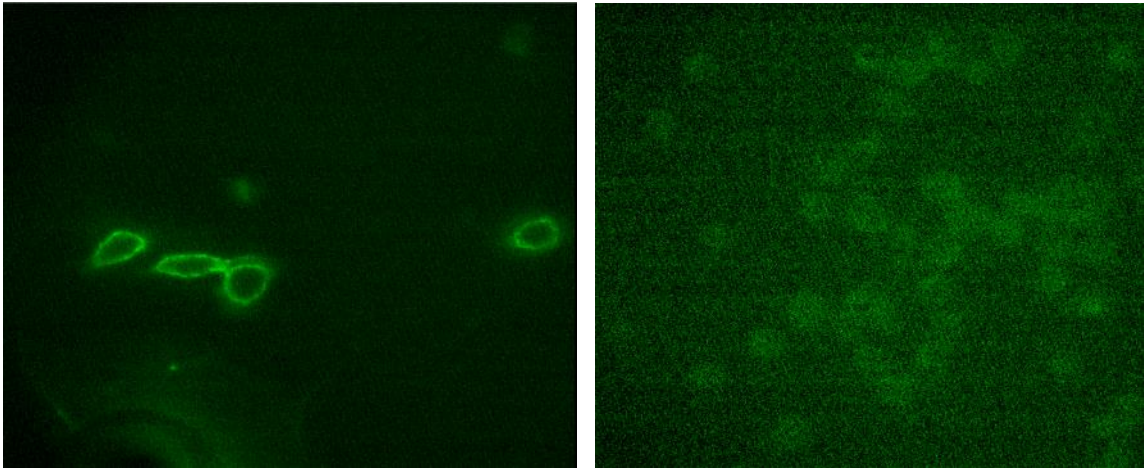


Figure 4.4 On the left cells labeled with a 1:100 dilution of A488 α -TLR4 imaged on spinning disk confocal microscope. On the right are the unlabeled control cells showing the autofluorescence.

Samples were imaged with a spinning disk confocal demonstrating successful labeling of the cellular membrane after 30 minutes incubation on ice. The next experiment utilized a 1:100 dilution of A488 α -TLR4 on cells after incubation with *E. coli* LPS for different amounts of time. No labeling was seen. Troubleshooting included introduction of a buffer comprised of PBS (to provide balanced salts and pH to the cells), non-fat dried milk and fetal goat serum (to serve as blocking agents to non-specific antibody binding), but there was still no significant signal to be seen when samples were imaged again with the spinning disk confocal. Once again, samples were analyzed with hyperspectral microscopy. These experiments demonstrated a low level of A488 spectra on the cell membrane, but showed that cellular autofluorescence in the 488 channel was masking this signal. To compensate, a much lower dilution of A488 α -TLR4 (1:25) was used in subsequent labelings of cells.

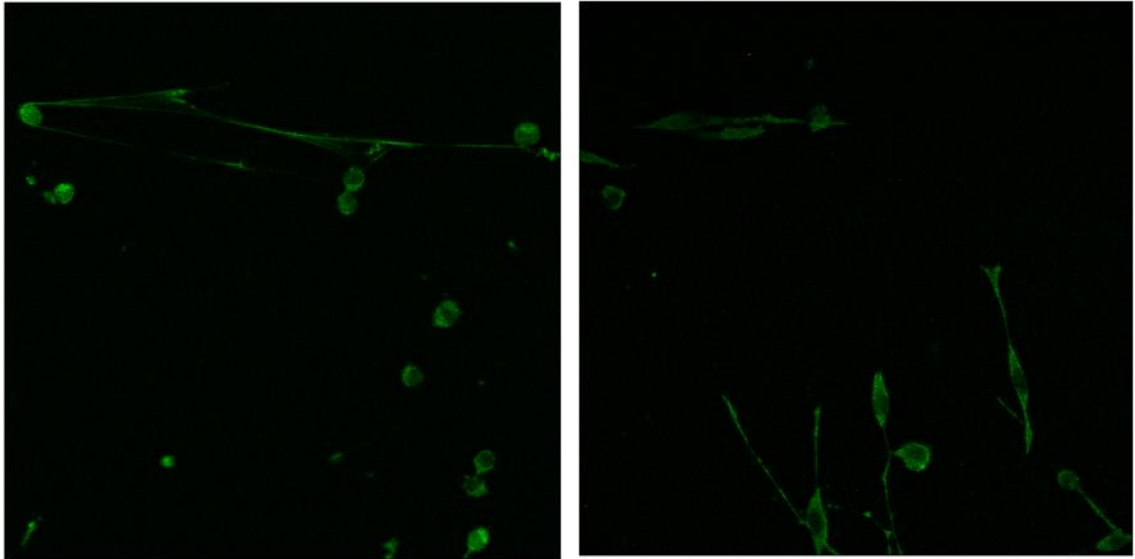


Figure 4.5 On the left cells labeled with a 1:25 dilution of 488 labeled antibodies imaged on laser scanning confocal microscope. On the right are the unlabeled control cells showing the autofluorescence.

Although labeling was slightly enhanced, there was still not sufficient signal to make any determinations about TLR4 internalization during LPS time course experiments, so a new α -TLR4 antibody from Abcam was ordered (ab22048).

4.3 Alexa Fluor 568 Labeled Antibody

The new α -TLR4 antibody was labeled with Alexa Fluor 568 (Life Technologies) following manufacturer protocols. Alexa Fluor 568 was chosen because the P388D1 cells had lower autofluorescence in the Alexa Fluor 368 emission wavelength. Cells were labeled on ice, as previously, for 30 minutes, and imaged through an 100x objective on a widefield, upright

microscope. Sufficient label was detected and experiments proceeded to labeling of cells after time course incubation with either *E. coli* or *Y.pestis* 37C LPS. Images were taken and analyzed for TLR4 internalization.

Cells were reacted with 100 nM *E. coli* LPS and then labeled with a 1:200 dilution of α -TLR4 A568 (degree of labeling on the antibody was 6 A568:1 antibody). After fixation, cells were imaged with widefield on a 100x oil objective using gain of 3 and a 300 ms exposure.

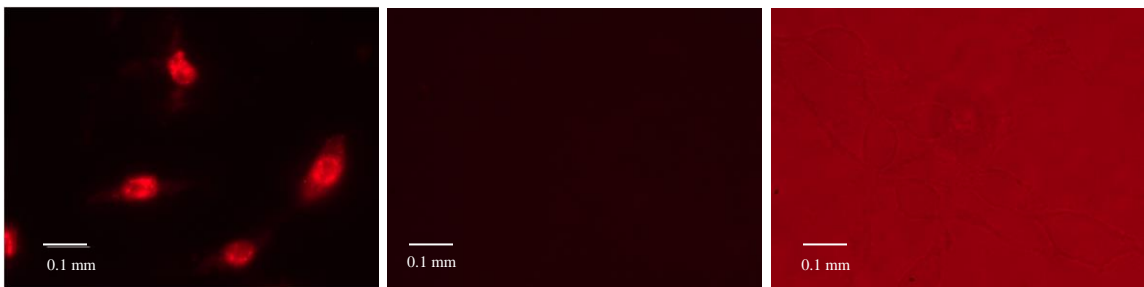


Figure 4.6 From left to right: A. P388D1 cells reacted with *E. coli* LPS for one hour and labeled with 568 antibody. These cells were imaged on the upright microscope. B. Control cells imaged on upright microscope to determine the amount of autofluorescence contributing to the signal. C. DIC image of control cells imaged on upright microscope to determine the amount of autofluorescence contributing to the signal.

To determine autofluorescence, unlabeled cells were imaged with the same parameters with the TRITC filter (see Figure 4.6 B) and in DIC (see Figure 4.6 C) to delineate where the cellular edges were.

P388D1 cells were also incubated with *Y. pestis* 21C LPS to determine if TLR4 internalization varied from that seen with *E. coli* LPS. New α -TLR4 A568 was generated for these experiments with a degree of labeling of 4:1. To compensate for the lower degree of

fluorescence with the new batch of α -TLR4 A568, a lower dilution (1:100) was used in labeling experiments, gain was raised to 12, and the exposure time was increased to 750 ms.

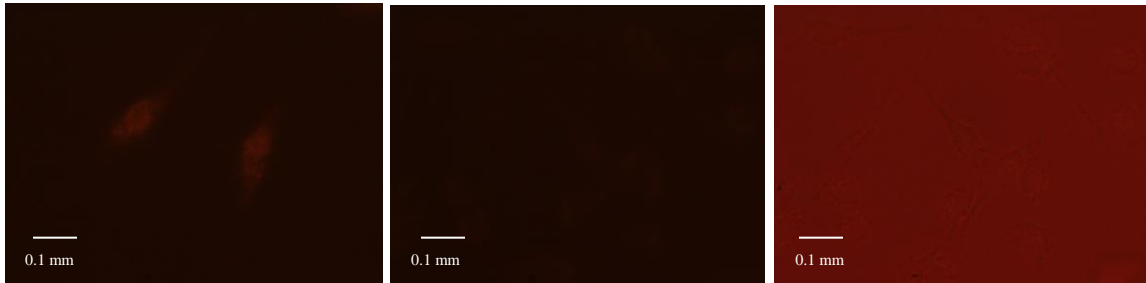


Figure 4.7 From left to right: A. P388D1 cells incubated with *Y. pestis* 21C LPS for one hour and labeled with α -TLR4 A568 and imaged on an upright widefield microscope with an oil 100x objective. B. Control cells were treated similarly as samples labeled with α -TLR4 A568 and imaged using the same conditions to determine levels of autofluorescence. C. DIC image of control cells to determine where the cellular membrane is when calculating autofluorescence.

30 cells were imaged for each LPS incubation time point and post image analysis (described in Figure 4.7) was performed to subtract both autofluorescent and background signal. The percent internalization was then plotted against time exposed to LPS (See Figure 4.8).

Internalization of Labeled anti-TLR4 Antibody

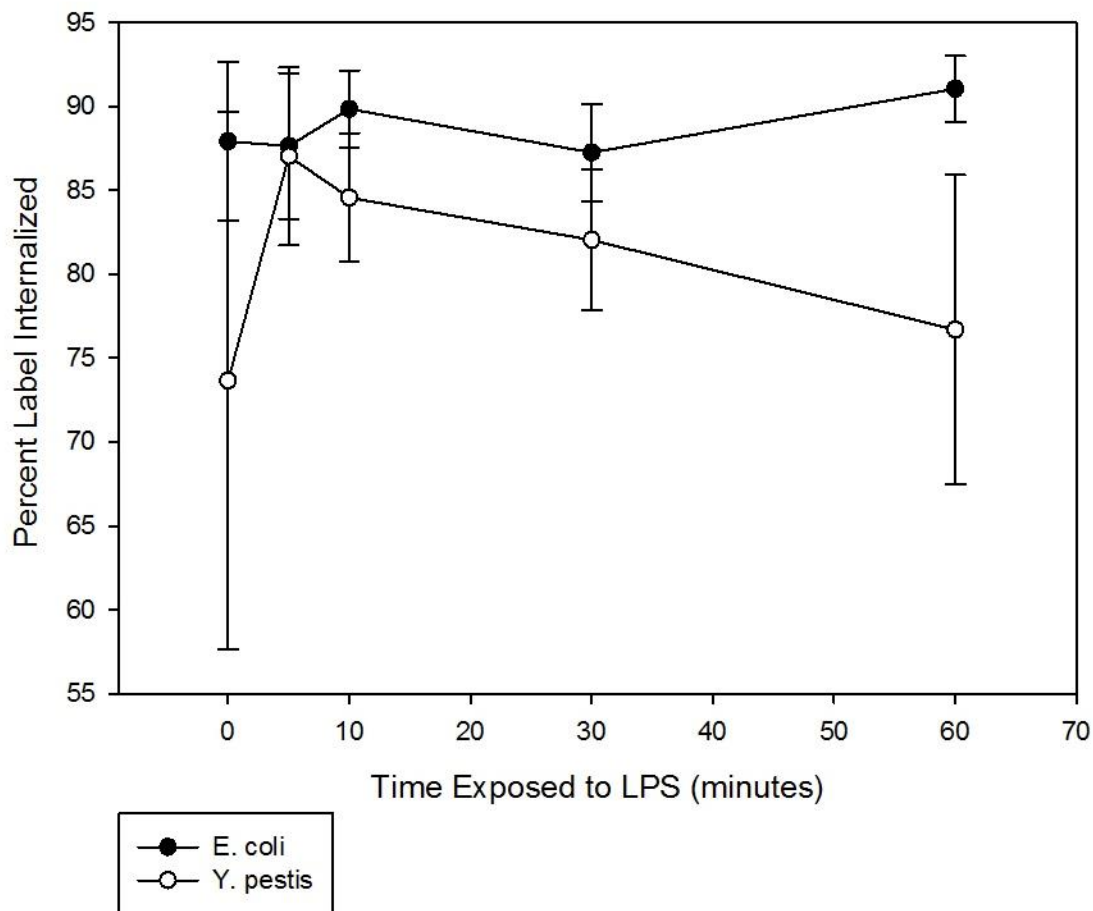


Figure 4.8 Rate of LPS internalization for *E. coli* and *Y. pestis* 21C.

These experiments looked at the evolution over time of internalization of the TLR4. Cells incubated with *E. coli* LPS for 60 minutes showed the highest amount of internalization at 91.04±1.97 percent internalization. Cells incubated with *Y. pestis* 21C LPS peaked at 5 minutes with an 87.04±5.30 percent internalization. The error bars were the standard deviation from the percent internalized for 30 cells at that time point. These results show no statistically significant

trends as the error bars overlap one another. Furthermore, the *E. coli* trial at time 0 shows close to 90 percent of the label inside the cell. The chart should show almost no label inside the cell at time 0. By time 30, around 60% of the label should be internalized. [19] The data collected in this time course contradicts this current data in the field, indicating an issue with the experiment and/or post processing. Overall, the results from these experiments are inconclusive.

Chapter 5

Discussion

Initial tests with laser scanning confocal microscopy, spinning disk confocal microscopy, and TIRF microscopy were all essential. Imaging with these microscopes identified problems with the labeling and autofluorescent signal from the cells. Difficulties experienced with experiments utilizing confocal and TIRF microscopy appeared to be due to technical issues ranging from low/no antibody binding, poor signal to background ratio, and problems with P388D1 cells at high passage number. The preliminary data described in this report will benefit from repeat with use of confocal and TIRF microscopy techniques to re-analyze the rate of TLR4 internalization upon incubation with different types of LPS for different amounts of time. The laser scanning confocal microscope will allow for more precise imaging of a single plane of the cells (as compared to wide-field microscopy), and TIRF will serve to delineate more clearly TLR4 localization in the membrane (at least near the coverslip surface).

There were a few discrepancies between the biological samples imaged. The cells exposed to the *E. coli* LPS were on passage 2, while the cells exposed to the *Y. pestis* 21 degree Celsius LPS were on passage 18. Another difference between the biological samples was the antibodies. The antibodies used in the *E. coli* trials had a degree of label of 6.1 and a dilution of 1:200. The antibodies used in the *Y. pestis* 21 trials had a degree of label of 4.05 and a 1:100 dilution. In order to view the antibodies at the same level of brightness, the exposure time and gain were changed. In the *E. coli* trials the exposure was 300 ms, while the gain was 3. The *Y. pestis* 21 trials had an exposure 750ms and a gain of 12. Variation between samples due to

differences in cellular passage number and antibody degree of labeling are not expected to contribute significantly to the overall level of TLR4 internalization. Repeating these experiments with the P388D1 and another macrophage cell line, such as RAW264.7, will serve to demonstrate that this is the case.

The results for the *E.coli* and *Y. pestis* trials were inconclusive. The values for label inside the cell without LPS stimulation were too high in comparison with other research in the field [19], furthermore, the time course showed no statistically significant trends of TLR4 internalization throughout the different time points. The methods for setting the thresholds most likely excluded too many of the membrane label points and not enough of the internal autofluorescence. This lead to the indication that all the labeled TLR4 was already inside the cell prior to LPS exposure.

Chapter 6

Conclusion and Future Experiments

The results of these experiments were inconclusive. Therefore, these experiments will need to be repeated with some alterations to protocol, as well as need to be performed with non-stimulatory *Y. pestis* 37C LPS to characterize differences in TLR4 internalization rates in response to stimulation with different types of LPS. This data will lead into dSTORM imaging of the TLR4 receptor in the membrane as previous experiments indicate that TLR4 clusters should have adequate time react in cells exposed to *E. coli* or *Y.pestis* 21C LPS for 30 minutes. [2]

Ideally, repetition of the experiments described herein will utilize a variety of macrophage lines (P388D1 and RAW264.7) on the same passage number with the same α -TLR4 antibody so that age of cells and degree of labeling will not factor into the results. Current results are calculated from analysis of 30 cells from each timepoint. Future experiments will benefit from multiple trials with analysis of similar numbers of cells. Additionally, analysis of TLR4 internalization upon stimulation of cells with *Y. pestis* 37C LPS (a non-stimulatory LPS) will allow for comparison of TLR4 dynamics relative to the stimulatory ability of the LPS. These experiments will benefit from the use of TIRF and dSTORM as well, to allow for super-resolution analysis of TLR4 in the membrane.

While wide-field microscopy was beneficial and sufficient for the experiments detailed in this thesis, use of confocal microscopy will serve to enhance the data. The application of the confocal pinhole to the fluorescent signal in these samples will aid in separation of autofluorescent and fluorescent signal from α -TLR4 labeling. The inclusion of membrane labels

and/or nucleus labels will aid in the determination of what α -TLR4 label is truly internal to the cellular membrane. Another possible study would determine if fluorescent label on the α -TLR4 antibody is affected by internalization (due to decreased pH found in lysosomes) such that the label becomes cleaved or degraded and is no longer representative of TLR4 localization. The results described in this thesis serve as a starting point for analysis of TLR4 internalization in response to different types of LPS. Future experiments will further clarify TLR4 dynamics, both on the membrane and during internalization, to demonstrate how TLR4 signaling occurs upon stimulation.

REFERENCES

- [1] Y.-C. Lu, Y. Wen-Chen, S. Ohashi S., "LPS/TLR4 signal transduction pathway," *Cytokine*, pp. 145-151 (2008).
- [2] J.S. Aaron, B. D. Carson, J.A. Timlin, "Characterization of Differential Toll-like Receptor Responses below the Optical Diffraction Limit," *Small*, pp 3041-3049 (2012).
- [3] Miyake, Kensuke, "Innate immune sensing of pathogens and danger signals by cell surface Toll-like receptors," *Seminars in Immunology*, 19(1), pp. 3-10 (2007).
- [4] Olympus Corporation. (2004). *Anatomy of the Fluorescence Microscope*. Retrieved August 24, 2013, from Microscope Resource Center:
<http://www.olympusmicro.com/primer/techniques/fluorescence/anatomy/fluoromicroanatomy.html>
- [5] Andor. (n.d.). *Spinning Disk Confocal*. Retrieved August 24, 2013, from
<http://www.andor.com/learning-academy/spinning-disk-confocal-a-technical-overview>.
- [6] Olympus Corporation. (2004). *Introduction to Confocal Microscopy*. Retrieved August 24, 2013, from Theory of Confocal Microscopy:
<http://www.olympusconfocal.com/theory/confocalintro.html>.
- [7] Nikon. (2000). *Numerical Aperture*. Retrieved August 24, 2013, from MicroscopyU:
<http://www.microscopyu.com/articles/formulas/formulasna.html>.
- [8] Nikon. (2000). *The Diffraction Barrier in Optical Microscopy*. Retrieved August 24, 2013, from MicroscopyU:
<http://www.microscopyu.com/articles/superresolution/diffractionbarrier.html>.
- [9] L. Schermelle, R. Heintzmann, H. Leohardt, "A guide to super-resolution fluorescence microscopy," *J. Cell Biol.*, pp. 165-175 (2010).
- [10] Nikon. (2000). *Total Internal Reflection Fluorescence (TIRF) Microscopy*. Retrieved August 24, 2013, from MicroscopyU:
<http://www.microscopyu.com/articles/fluorescence/tirf/tirfintro.html>.
- [12] M. Schuttpelz, S. Wolter, S. van de Linde, M. Heilemann, M. Sauer, "dSTORM: real-time subdiffraction-resolution fluorescence imaging with organic fluorophores," *Single Molecular Spectroscopy and Imaging III* (2010).
- [13] M. Sauer, M. Heilemann, "Super-Resolution Fluorescence Imaging of Cellular Structures and Dynamics with Conventional Fluorophores," *Imaging & Microscopy* (2010).
- [14] M. Heilemann, S. van de Linde, T. Klein, M. Sauer, "Live-Cell Super-Resolution with dSTORM," *Imaging & Microscopy* (2011).
- [15] S. van de Linde, A. Loschberger, T. Klein, M. Heidbreder, S. Wolter, M. Heilemann, et al., "Direct stochastic optical reconstruction microscopy with standard fluorescent probes," *Nature Protocols*, pp. 991-1009 (2011).
- [16] Darveau and Hancock, *J. Bacteriology*, 155(2), pp. 831-838 (1983).
- [17] W. S. Rasband, ImageJ, U.S. National Institutes of Health, Bethesda, Maryland, USA, <http://imagej.nih.gov/ij/>, 1997-2014.
- [18] P. Lepanto, F. Lecumberry, J. Rossello, A. Kierbel, "A confocal microscopy image analysis method to measure adhesion and internalization of *Pseudomonas aeruginosa* multicellular structures into epithelial cells," *Molecular and Cellular Probes*, 28, pp. 1-5 (2014).
- [19] I. Zanoni, R. Ostuni, L.R. Marek, S. Barresi, R. Barbalat, G. M. Barton, F. Granucci, J. C. Kagan, "CD14 Controls the LPS-Induced Endocytosis of Toll-like Receptor 4," *Cell*, 147, pp. 868-880 (2011).